Design of an Imaging Telescope with Variable Magnification and

Imaging Distance

Eileen Norris

Brighton High School
1150 Winton Road, Rochester, NY

Advisor: Dr. Seung-Whan Bahk

Laboratory for Laser Energetics
University of Rochester, Rochester, NY

March 2016

Abstract

Vacuum spatial filters, used to control beam quality and remove unwanted high spatial frequency noise from amplified beam pulses, mostly rely on two-lens imaging telescopes with no flexibility in magnification and imaging distance unless the lenses themselves are replaced. New three-lens and four-lens imaging telescopes facilitate adjustable beam magnification and imaging distance by altering only lens positions. Systems of ray matrices were constructed for three-lens and four-lens systems. This formalism determines the required adjustments of lens positions and can be used to predict and analyze beam magnification and imaging distance. Constraints, primarily fixed positions of lenses that are not moved, were set to maximize the convenience of the lens systems, confirming that for a range of magnification, not all lenses need to be moved when optimized initial focal lengths are used. A more detailed ray tracing program was created to model the new designs, verifying ray matrix calculations and revealing a peak-to-valley wave front error of typically 0.02 to 0.05 waves. Experimentally tested three-lens systems presented magnifications with a maximum deviation of 2.3% from the calculated values, confirming the calculations.

I.   Introduction

Vacuum spatial filters are used frequently at the Laboratory for Laser Energetics (LLE) to relay system image planes and remove unwanted high spatial frequency noise from amplified pulses. Figure 1 shows a common vacuum spatial filter assembly. Prior to this work, vacuum spatial filters at LLE have relied primarily on two-lens imaging telescopes. While the collimation of the beam can be adjusted with small shifts in lens positions, the magnification and imaging distance of these two-lens systems can only be changed by altering the focal lengths of the lenses, and therefore replacing the lenses themselves.
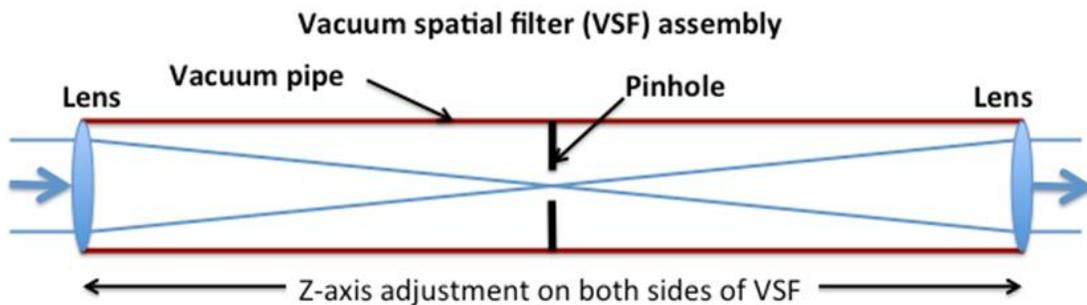
Figure 1: Schematic of a spatial filter. A pinhole is used to remove high spatial frequency noise from the amplified pulses and the lenses are adjusted along the z-axis to maintain beam collimation.[1]

New three-lens and four-lens imaging telescope designs, however, facilitate adjustable beam magnification and imaging distance by altering only lens positions. This report describes the use of ray matrix formalism and experimental setups to determine and verify a three-lens optical system enabling variable magnification and imaging distance.

II.   Three-Lens System

First, we produced a three-lens design [Figure 2]. Based on the ray matrix formalism shown in Sec. III, the position of the first lens (F1) is fixed in this design with the distance labeled D1

also fixed. Fixing the first lens position provides the advantage of fixing the location of the spatial-filtering pinhole. While the positions of F2 and F3 are adjustable within the system, the total length of the system (L = D1+D2+D3+D4) can be set for a given system, but once set, is immutable for the remainder of the calculations for that system. The plane on the left of Fig. 2 is imaged onto the plane on the right.
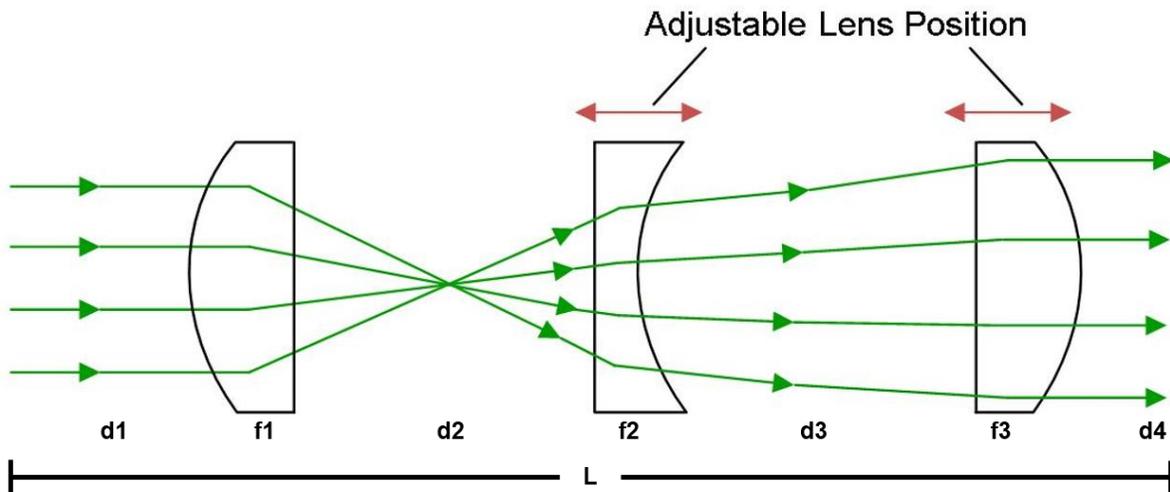
Figure 2: Schematic of the propagation of a beam through the proposed three-lens system. The first lens, F1, is fixed, and F2 and F3 are adjustable. The total length of the system, L, is also fixed. The ray paths are shown schematically; in reality the ray paths are refracted outward by the center lens F2.

As in conventional laser-beam imaging systems, the system is designed to be comprised of plano convex and plano concave lenses. The first and third lenses, F1 and F3, are plano convex, and the center lens is plano concave. Due to anticipated lab constraints, the positions of the lenses in the system were optimized for a specific set of lens focal lengths.

III.   Ray Matrix Formalism

Lens systems can be modeled with paraxial ray matrix formalism and a more comprehensive three-dimensional ray tracing model. A paraxial ray can be defined as a ray which is close enough to the optical axis of a system that sines of angles between the rays and the optical

axis may be replaced by the angles themselves in calculations. The change in position and inclination of a paraxial ray through an optical system can be represented by paraxial ray matrices.[2] For this experiment, the behavior of an optical ray can be separated into two scenarios: through free space and through a thin lens. The propagation of an optical ray in free space is given by

$$\begin{bmatrix} r` \\ \theta` \end{bmatrix} = \begin{pmatrix} 1 & d \\ 0 & 1 \end{pmatrix} \begin{bmatrix} r \\ \theta \end{bmatrix} \tag{1}$$

where d is the distance the ray is traveling through free space, r and r` are the initial and final distances of the ray from the optical axis, respectively, and $\theta$ and $\theta`$ are the initial and final angles of the ray with respect to the optical axis, respectively.

The propagation of an optical ray through a thin lens is given by

$$\begin{bmatrix} r` \\ \theta` \end{bmatrix} = \begin{pmatrix} 1 & 0 \\ -1/f & 1 \end{pmatrix} \begin{bmatrix} r \\ \theta \end{bmatrix} \tag{2}$$

where f is the focal length of the lens and r [r`] and $\theta$ [$\theta`$] are the same parameters used in Eq. (1). It should be noted that we used the thin lens approximation for each lens in the system in our initial ray matrix calculations. This approximation ignores the optical effects associated with finite lens thicknesses and therefore simplifies ray tracing calculations. In reality, the lenses used to model and construct the three- and four-lens systems are 2-3 mm in center thickness. This thickness is considered in the more complex ray tracing program as described in Sec. IV.

Ray transfer matrices can be multiplied together in sequence to obtain an overall ray transfer matrix for the optical system – lens and free-space components together. It is important to note that this matrix multiplication is not commutative, so the matrices must be ordered according

to the setup of the optical system. Thus, the behavior of a ray through an optical system of both

lens and free space components can be given by

$$\begin{bmatrix} r^{`} \\ \theta^{`} \end{bmatrix} = \begin{pmatrix} A & B \\ C & D \end{pmatrix} \begin{bmatrix} r \\ \theta \end{bmatrix} \quad (3)$$
,

where the matrix [A, B, C, D] is the product of matrices describing the individual components of

the optical system. By the rules of matrix multiplication, we know that

$$r^{`} = Ar + B\theta \quad (4)$$

The imaging condition set on the optical system states that the displacement of the ray through the

optical system from the optical axis does not vary with the initial angle θ (i.e. all rays from a point

in the object plane pass through the same point in the image plane), requiring B = 0 because r` is

independent of θ.

Through matrix multiplication, we also know that

$$\theta^{`} = Cr + D\theta \quad (5)$$

The collimation condition set on the optical system states that the angle $\theta^{`}$ of the optical

ray is independent of the displacement of the ray. If the beam enters the system collimated – that

is, the ray bundles are all parallel – it will exit the system collimated. Therefore, C = 0.

When the beam is collimated and imaged, the ratio of beam sizes (r`/r) or the ratio of

angular divergences (θ/ $\theta^{`}$) is the magnification of the system. From Eqs. (4) and (5), we infer that

$$A = \frac{1}{D} = M < 0 \quad (6)$$
,

where M is the magnification, which is negative because the image is reversed.

Assuming these three conditions, ray matrix algebra can be easily performed in

Mathematica. The free space and thin lens components can be multiplied in sequence to obtain the

overall ray transfer matrix for the optical system. This ray transfer matrix, accepted imaging and collimation conditions, and controlled focal lengths and total system length can be used to solve the distances at which the three lenses in the system are located versus the desired magnification of the system. Eqs. (7) – (17) represent ray matrix algebra performed in Mathematica. First, the propagation of a lens through free space and a thin lens, as seen in Eqs. (1) and (2), is defined by

$$\mathbf{DFree} = \begin{pmatrix} 1 & d \\ 0 & 1 \end{pmatrix} \tag{7}$$

$$\mathbf{DLens} = \begin{pmatrix} 1 & 0 \\ -1/f & 1 \end{pmatrix} \tag{8}$$

The overall ray transfer matrix was then calculated by multiplying the individual components of the three-lens system in respective order, given by

$$\mathbf{DFree[D4] \cdot DLens[F3] \cdot DFree[D3] \cdot DLens[F2] \cdot DFree[D2] \cdot DLens[F1] \cdot DFree[D1]} = \begin{pmatrix} A & B \\ C & D \end{pmatrix} \tag{9}$$

Assuming the conditions given in Eqs. (4) – (6), a system of equations was written, stating

$$\mathbf{A = M} \tag{10}$$

$$\mathbf{B = 0} \tag{11}$$

$$\mathbf{C = 0} \tag{12}$$

$$\mathbf{D1 + D2 + D3 + D4 = L} \tag{13}$$

This system of equations, and the previously defined overall ray transfer matrix in Eq. (9), were used to solve for D1, D2, D3, and D4, with respect to the focal lengths (F1, F2, and F3), magnification (M), and total length of the system (L). D1, D2, D3, and D4 are given by

$$\mathbf{D1} = \frac{F2^2F3^2 + F1^2F2F3M + 2F1F2^2F3M + 2F1F2F3^2M - F1F2F3LM + F1^2F2^2M^2 + F1^2F3^2M^2 + F1^2F2F3M^3}{F1F2F3(-M+M^3)} \tag{14}$$

$$D2 = \frac{F1F3 + F2F3 + F1F2M}{F3} \tag{15}$$

$$D3 = \frac{F2F3 + F1F2M + F1F3M}{F1M} \tag{16}$$

$$D4 = \frac{-F1F2F3^2 - F1^2F3^2M - F2^2F3^2M - 2F1^2F2F3M^2 - 2F1F2^2F3M^2 - F1F2F3^2M^2 + F1F2F3LM^2 - F1^2F2^2M^3}{F1F2F3(-1+M^2)} \tag{17}$$

Once the positions of the lenses were related to the focal lengths, magnification, and length of the optical system, specific focal lengths and the desired length of the system could be entered, therefore leaving lens position as a function of magnification. We then graphed lens positions versus the magnification [Figure 3].
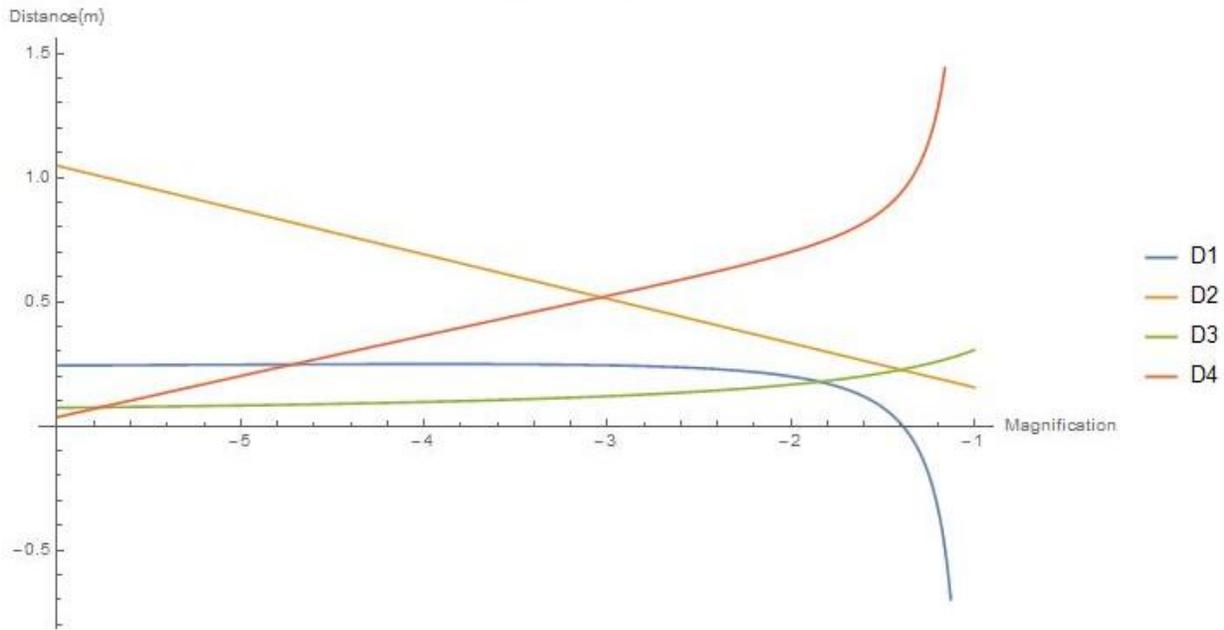
Figure 3: Graph of lens position (D1, D2, D3, D4) versus magnification. F1 = 200 mm, F2 = -223 mm, F3 = 250 mm, L = 1.4 m. Note that the graph of D1 is relatively flat across a wide range of magnifications while the graphs of D2, D3, and D4 are more variable.

Because the graph of D1 is relatively flat, we determined that D1 can be set at a constant position, as shown in the three-lens design of Fig 2. In the case of Figure 3, for F1 = 200 mm, F2 = -223 mm, F3 = 250 mm, and L = 1.4 m, the first lens (F1) can be set at a constant position of

approximately 0.25 m. For different sets of focal lengths and total lengths of the system, the graph of D1 remains relatively flat over a wide range of magnifications. The three-lens design therefore functions for a range of lens focal lengths and desired total lengths.

IV.   Ray-Tracing Simulations

After solving for the distances between the lenses as a function of magnification and showing that D1 can be set at a constant value, a more complex program was written based on a MATLAB ray tracing code package.[3] This package allows modeling of the realistic aspects of the experiment such as the center thickness of the lenses (the thin lens approximation was used in the initial calculations), the material of the lenses – primarily fused silica and BK7 – and the aperture size and the radii of curvature of the lenses.

The equations obtained by Mathematica for the lens positions [Eqs. (14) – (17)] were transferred into the MATLAB ray tracing program, which further analyzed the beam's behavior through the three-lens system. This MATLAB ray tracing program performs three dimensional ray tracing including lens material and thickness. The distances found in Mathematica were transferred as the distances between the first surfaces of each optical element in the system.

A detector plane placed at the end of the optical system in the program enables further analysis of the wavefront and beam distribution at the end of the system. Our program gives three primary outputs: three-dimensional traces of the optical rays through the system, wavefront at the detector plane, and distribution of the beam rays on the detector plane.[3] Figures 4(a) and 4(b) show the propagation of the rays through the three-lens system for two magnifications.

(a)   **(b)**
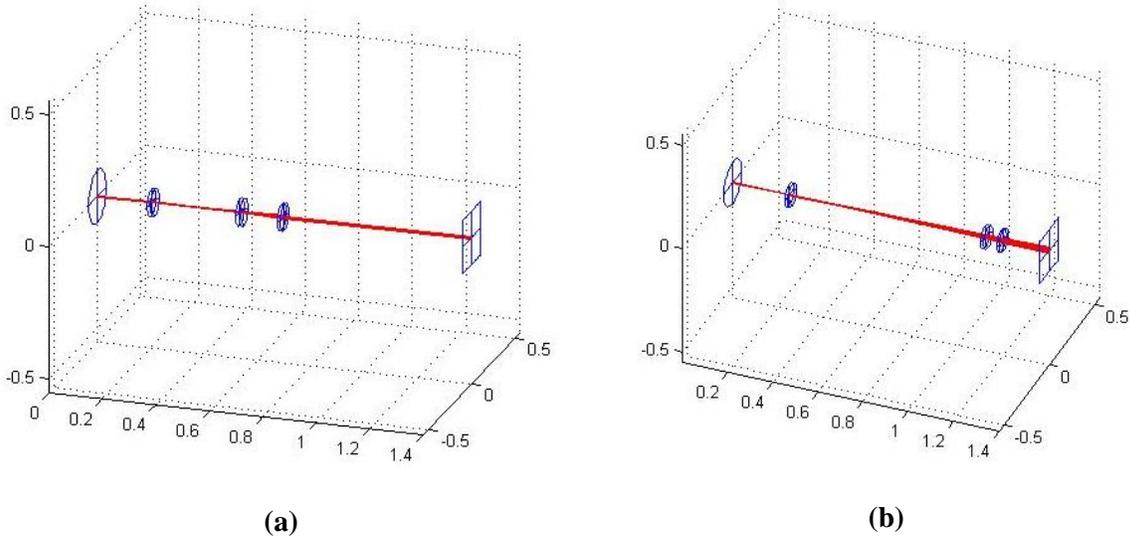
Figure 4(a): Propagation of a ray through a three-lens system with magnification -2. F1 is located at a distance D1, 0.247 m from the initial reference plane on the left. F1 = 200 mm, F2 = -223 mm, and F3 = 250 mm. The total length of the system (L) is 1.4 meters.
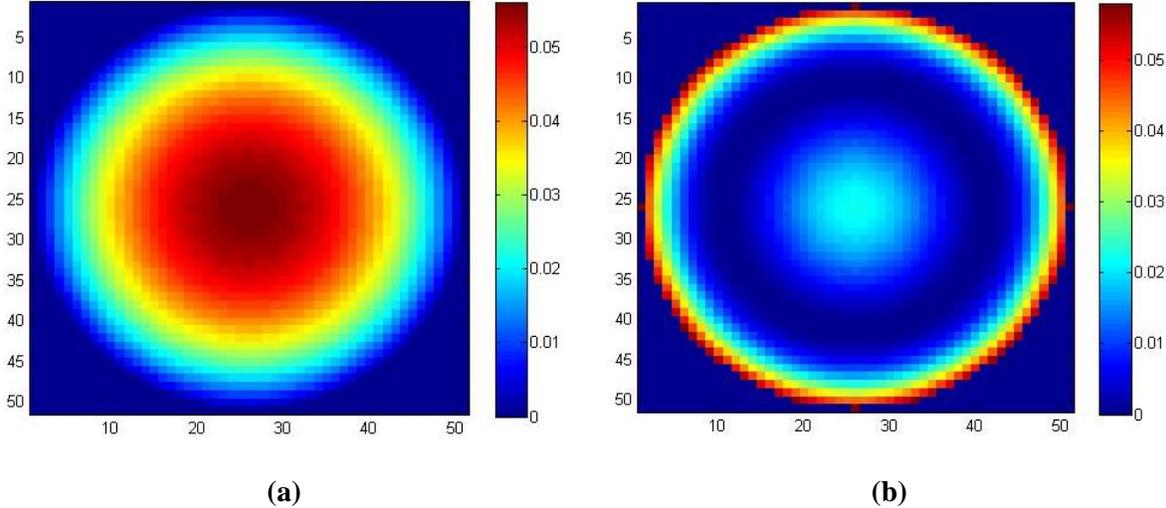
Figure 4(b): Same as Figure 4(a) except with a magnification of -5. Note that the position of F1 remains the same, with D1 = 0.247 m, and the total length of the system remains at 1.4 m. The change in magnification is enabled by the shifting in position of F2 and F3.

The MATLAB model of the propagation of a beam through the three-lens system confirms that F1 can be held in a relatively constant position. As seen in Figs. 4(a) and 4(b), over a wide range of magnifications, the distance of F1 from the reference plane remains the same. Therefore, for a given total length of the system and preset focal lengths of the lenses, the positions of the second and third lenses, F2 and F3, can change the magnification achieved by the system.

The MATLAB program, however, was used primarily to verify small wavefront error as the rays exit the system. Figs. 5(a) and 5(b) show the wavefront of the beam at the detector plane located at the end of the three-lens system for the two cases shown in Fig. 4.

(a)   **(b)**

Figure 5(a): Wavefront of the beam at the detector plate through a three-lens system with magnification -2. Shown on the scale to the right, the maximum wavefront error is 0.05 waves.
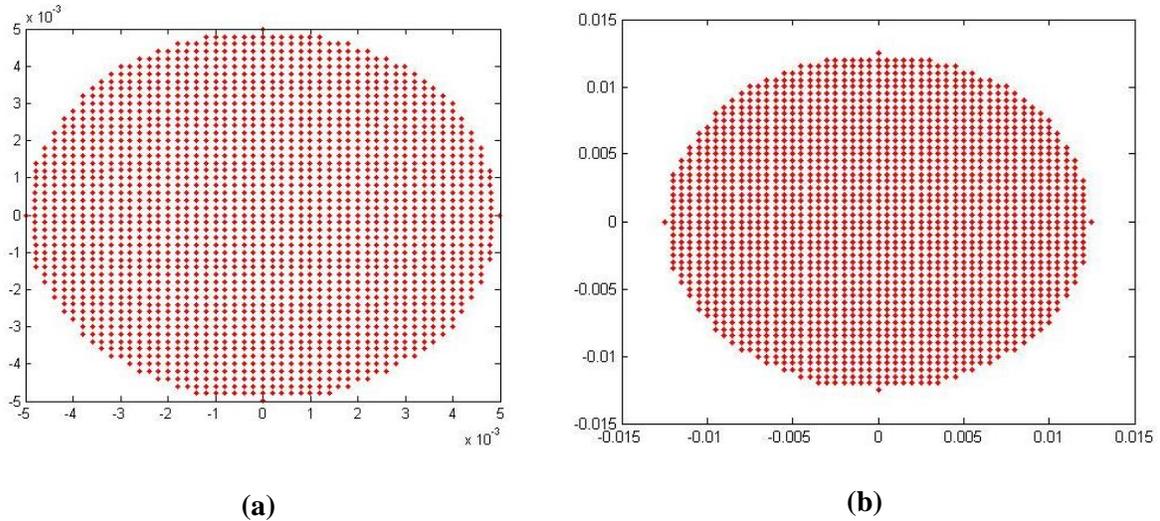**Figure 5(b):** Same as Figure 5(a) except with a magnification of -5.

The peak-to-valley (p-v) wavefront error, the maximum displacement, measured in waves, of the actual wavefront from the desired flat wavefront, in both positive and negative directions, is 0.05 in both cases shown in Fig. 5(a) and 5(b). A perfect lens or lens system is one that produces a wavefront with no aberrations, and therefore a zero p-v wavefront error. We use the Maréchal criterion[4] to set the upper limit on the acceptable wavefront error. This criterion sets the level of degradation of peak intensity of the imaged focal spot caused by the wavefront error to be within 20%. The corresponding allowable p-v wavefront error for a circularly symmetric system, in this case the spherical aberration, is less than 0.11 waves p-v. The typical wavefront error for the calculations performed in MATLAB is between 0.02 and 0.05 waves, confirming the acceptability of our three-lens design.

Figures 6(a) and 6(b) indicate the distribution of the beam rays across the detector plane.

(a)   (b)

Figure 6(a): Distribution of the beam on the detector plane through a three-lens system with magnification -2 and initial beam size 5 mm. The vertical and horizontal axes are shown in meters.
**Figure 6(b):** Same as Figure 6(a) except with a magnification of -5. Note that the scale changes.

Distributions of the beams on the detector planes were used to confirm the magnification by comparing the beam sizes before and after passing through the three-lens system.

V.   Experimental Verification

While the MATLAB ray tracing program is confirmed to give theoretically accurate lens positions, it is important to confirm that it parallels the behavior of a beam through our three-lens system accurately. The three-lens system modeled in the ray tracing program is easily transferrable into an experimental setup. Figure 7 shows the lab setup used to verify the accuracy of the MATLAB ray tracing program.
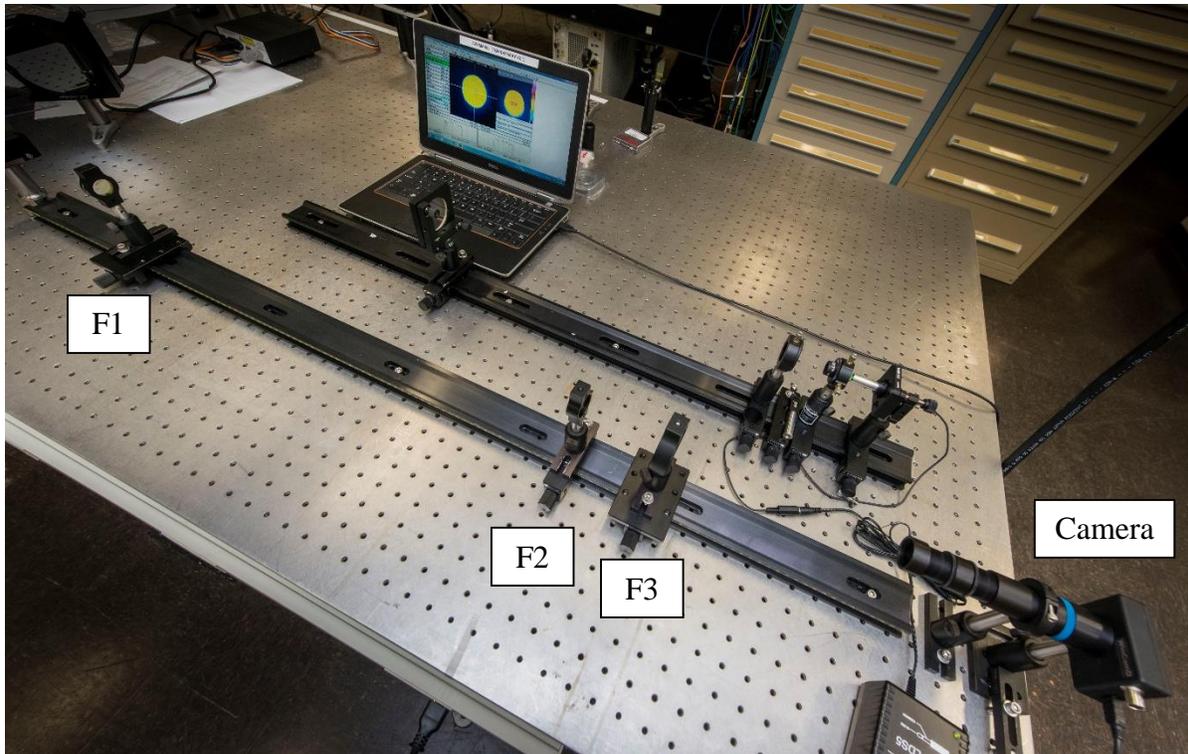
Figure 7: Lab setup of the three-lens system. The second and third lenses are on adjustable sliders. The system totals 1.4 m in length; however, note that due to table room constraints, the beam is bent in order to fit the system. The photo is taken by Eugene Kowaluk.

Limits exist in lens availability. Theoretically, based on the results of the MATLAB ray tracing program, the three-lens system will work with a wide range of focal lengths, providing that F1 and F3 are plano convex lenses, thus having positive focal lengths, and F2 is a plano concave lens with negative focal length. In this experiment, F1 = 200 mm, F2 = -223 mm, and F3 = 250 mm, as in Fig. 4. A nominal 2-mm aperture marks the beginning of the system, and controls the initial beam size entering the three-lens system. The beam size in our experiment, as set by the aperture, was measured to be 1.986 mm. The first lens was placed in a stationary position of 0.247 m from the aperture. This value was obtained from the graph of D1 in Mathematica, shown in Figure 3. Because the graph of D1 is relatively flat with respect to M at a value of approximately 0.247 m, we concluded that if F1 is held stationary, M can be controlled by adjusting only the

positions of F2 and F3. Experimentally, we tested this by placing a camera at the end of the three-lens system set up in the lab. This camera parallels the detector plane programmed into the MATLAB ray tracing program. Lenses F2 and F3 were shifted into their appropriate positions for specific magnifications, as determined by the MATLAB ray tracing program. Photographs of the beam's distribution on the camera lens were taken for each desired magnification. Figure 8(a) shows the images taken across a wide range of magnifications. Figure 8(b) shows corresponding lineouts of intensity versus pixels for each magnification.

M = -2.5

M = -3.5

M = -4.5

M = -5.5

(a)

(b)
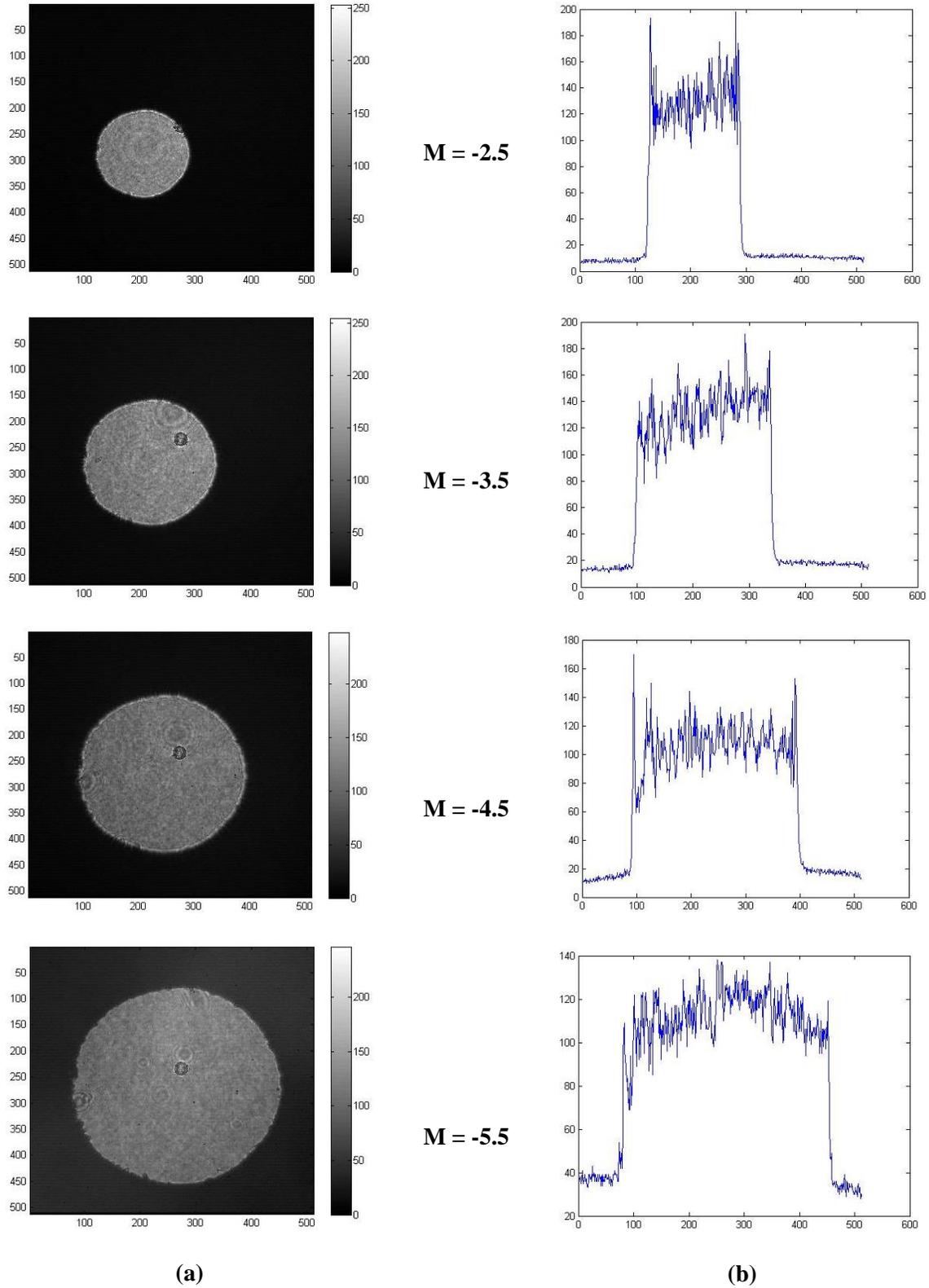
Figure 8(a): Distribution of the beam on the optical camera through a three-lens system over a range of magnifications. The initial beam size is 1.986 mm. The scale shows the beam intensity.

Figure 8(b): Corresponding lineouts of intensity versus pixels.

The images given in Figure 8(a) were used to confirm that the beam remains imaged as it exits the three-lens system and reaches the detection plane. If one looks closely at the images taken by the camera, the diffraction rings around the edge of the beam are minimal. A perfectly imaged beam will show no diffraction rings. However, because the rings in each of the images in Figure 8(a) can barely be seen, we can conclude that the beam was imaged adequately as it exited the system. The fact that the total image distance is maintained while varying the magnification is an important improvement over other variable magnification imaging systems. The state of output beam collimation and the residual spherical aberration in the system were not measured. This requires separate measurements of the input and output wavefronts using a wavefront sensor.

The lineouts of intensity versus pixels were used to further confirm the accuracy of the calculations made in the MATLAB ray tracing program. As shown in Figure 9, the full width at half max was taken on the graph for each magnification in order to determine the final experimental beam sizes. The experimental magnifications were calculated by relating the initial known beam size of 1.986 mm to the final
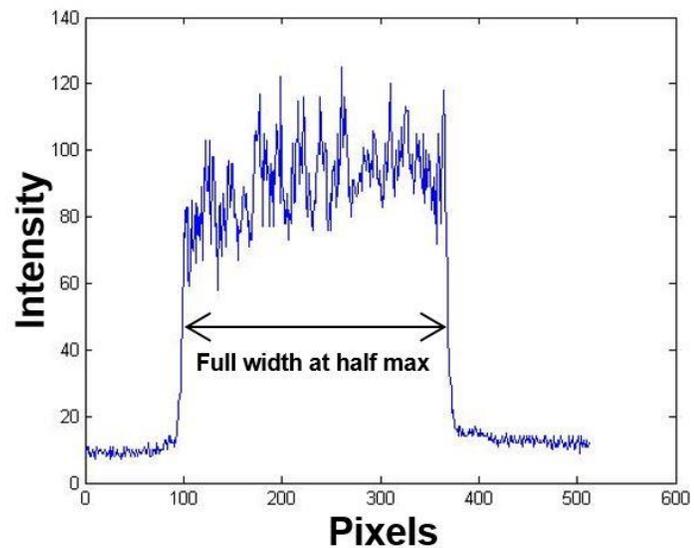
Figure 9: Lineout of intensity versus pixels at a magnification of -4. The full width at half max, the difference between the values of the independent variable at which the dependent variable is equal to half of its maximum value, is shown on the graph.

beam sizes determined by the full width at half max of the corresponding intensity lineout. The experimental and calculated magnifications, as well as percent deviations, are shown in Table 1.

M calculated	final beam size (mm)	M experimental	percent deviation
-2.5	5.03	-2.53	1.3%
-2.75	5.34	-2.69	-2.3%
-3	6.00	-3.02	0.7%
-3.25	6.31	-3.18	-2.3%
-3.5	7.01	-3.53	0.9%
-3.75	7.37	-3.71	-1.1%
-4	7.99	-4.02	0.5%
-4.25	8.38	-4.22	-0.7%
-4.5	9.00	-4.53	0.7%
-4.75	9.31	-4.69	-1.3%
-5	9.97	-5.02	0.4%
-5.25	10.54	-5.31	1.1%
-5.5	11.03	-5.55	1.0%

Table 1: Calculated magnifications, final beam sizes, experimental magnifications, and percent deviation from the calculated magnifications. Note that the maximum percent deviation was 2.3% in magnitude.

Figure 10 shows the magnification as a function of D2. This variable had the widest range of values; although all of D2, D3, and D4 were adjusted to achieve varied magnifications throughout the experiment, the second lens was the most shifted lens.

Magnification vs. D2
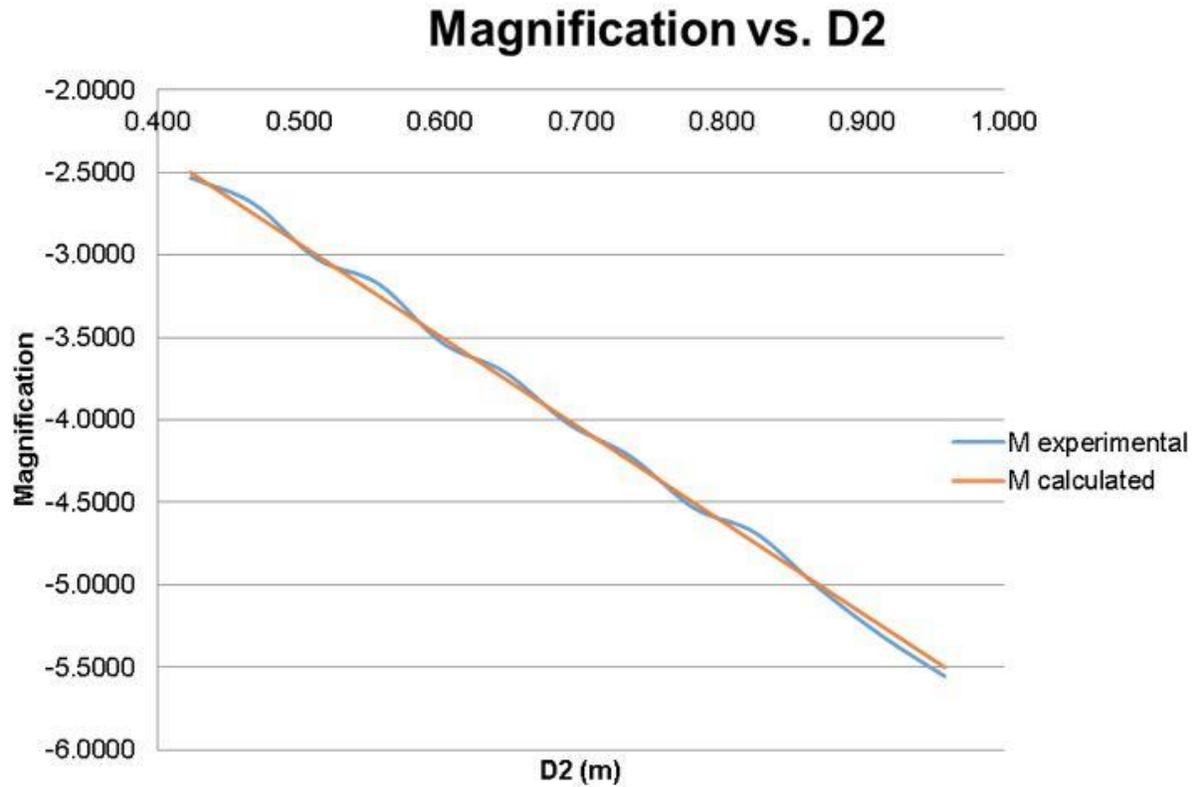
Figure 10: Graph of the experimental and calculated magnifications versus D2. There is little deviation of the experimental magnifications from the calculated magnifications. The maximum percent deviation is 2.3% in magnitude.

The comparison between the experimental and calculated magnifications was used to evaluate the accuracy of the MATLAB program in predicting the behavior of a beam through the three-lens system in a physical lab setting. With a maximum absolute error of 2.3%, we can confirm that the MATLAB ray tracing program and the equations derived in Mathematica can accurately give optimized positions for lenses in the three-lens system over a wide range of magnifications.

VI. Four-Lens System

A four-lens system was also considered and modeled similarly using the MATLAB ray tracing program. As shown in Figure 11, the two outer lenses are fully adjustable while the inner two lenses are set at fixed positions.
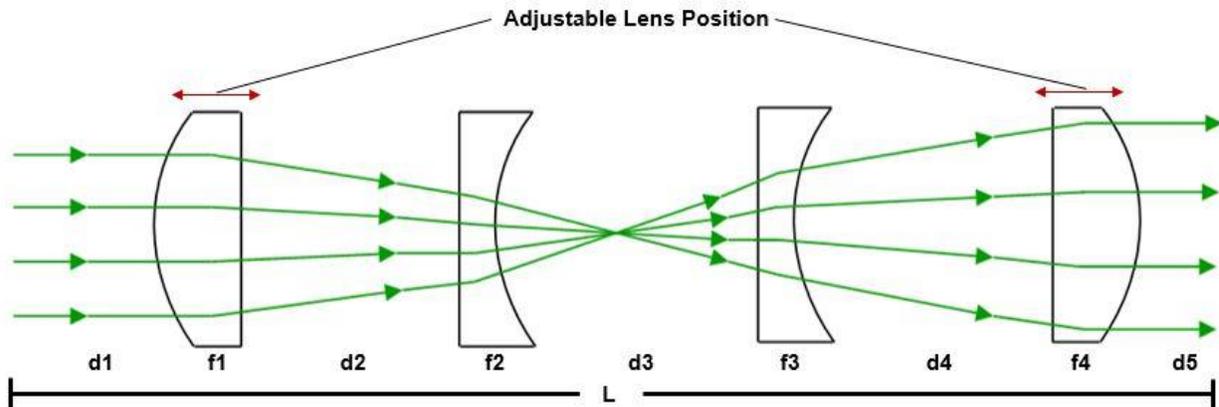
Figure 11: Propagation of a beam through a four-lens system. The inner lenses, F2 and F3, are fixed, and the outer lenses, F1 and F4, are adjustable. The total length of the system, L, is also fixed.

This four-lens system can be modeled in the same way as the three-lens system. As with the three-lens system, Mathematica was used to derive equations for the positions of the two outer lenses (D1, D2, D4, and D5). D3 remains constant because F2 and F3 are in fixed positions. The MATLAB ray tracing program was written to model this four-lens system at varying magnifications. Although we were unable to confirm the accuracy of these calculations experimentally, we can safely assume that, like the three-lens system, an experiment done with the four-lens system will not deviate significantly from the predictions made in MATLAB. This four-lens system enables a vacuum tube to be placed surrounding F2 and F3, although the focal plane might shift depending on other distances. With vacuum spatial filters being commonly used in

many of the labs at LLE, this new four-lens system enables variable magnification and imaging distance by changing only the positions of two outer lenses rather than altering lens focal lengths.

VII.   Conclusion

Three- and four-lens image relay telescopes were designed whose magnification and total imaging distance are adjustable by changing inter-lens distances only. Each optical system includes two adjustable-position lenses and at least one fixed lens to maximize utility. The positioning of the adjustable-position lenses in each system for specific desired magnifications and imaging distances can be analytically predicted through ray matrix calculations and can be further analyzed using a more complex MATLAB ray tracing program. In the case of the three-lens system, experiments using the lens positions given by the outputs of the ray tracing program confirmed the program's accuracy in determining lens positions for specific focal lengths, lens materials, and magnifications. Experimentally tested three-lens systems presented magnifications with a maximum deviation of 2.3% from the calculated values. Further experimentation with the four-lens system is expected to similarly confirm the accuracy of the MATLAB ray tracing program. Thus far, it appears that a three-lens system enabling adjustable magnification and total imaging distance merits serious consideration.

VIII.   Acknowledgements

giving me the opportunity to work at the lab. Finally, I would like to thank my family, friends, and fellow interns for their constant help and support throughout the program.

IX.   References

[1] "OMEGA EP System Operations Manual Volume VII–System Description Chapter 5: Optomechanical System," S-AD-M-009 (August 2007).

[2] A. Gerard and J.M. Burch. *Introduction to Matrix Methods in Optics*. New York: Dover Publications, 1975.

[3] Bahk, Seung-Whan. "Matlab Ray Tracing User Manual."

[4] M. Born and E. Wolf. "Principles of Optics." 6th edition (1980). Chapter 9.